

Effects of Loading History on the Behavior of Reinforced Concrete Columns

ACI 113: Open Topic Session, Part 1 of 2

Presenter: Sasan Dolati

Structural Engineer at  **Stantec**

Ph.D. Advisors : Adolfo Matamoros, Wassim Ghannoum



Outline

- ❑ Introduction
 - a) Problem statement and background
 - b) Objective and scope

- ❑ Part 1: Recommendations for Nonlinear Finite Element Analyses of Reinforced Concrete Columns Under Seismic Loading up to Collapse
 - a) Specimen configuration (material, loading, BC, mesh)
 - b) Experimental calibration
 - c) Simulation error

- ❑ Part 2: Loading History Effects on Drift Capacity of Reinforced Concrete Columns Under Seismic Loading
 - a) Simulations under various lateral protocols and axial loads
 - b) Parameters for drift capacity relations
 - c) Drift capacity relations
 - d) Proposed Drift Capacity Equations
 - e) Validation
 - f) Example application with ACI 369.1- ASCE 41-17 drift capacities

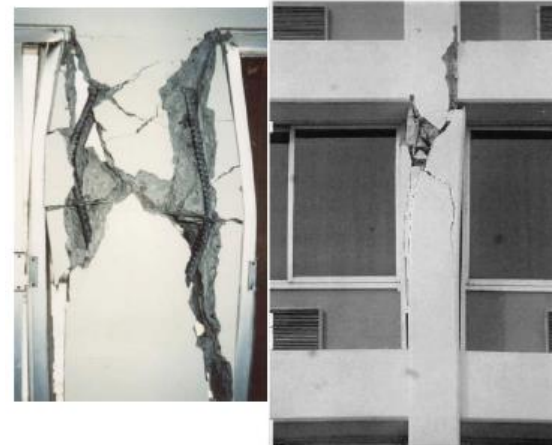
- ❑ Conclusion

Introduction

- ✓ Many existing concrete buildings do not satisfy the seismic collapse-prevention by current standard.
- ✓ Collapse of non-ductile concrete buildings mostly occur with loss of columns (light confinement).
- ✓ These columns in the US {
 - before 1970: in high seismic region. {
 - California: 20,000 to 23,000
 - currently: in low seismic region. {
 - Los Angeles: 1500 buildings, \$1.8 to \$28.5 billion and 8,300 fatalities
- ✓ Research shows that loading history is key parameter in column behavior and earthquake tends to impart different types of lateral histories



Collapse of second and third floor concrete column by earthquake



Holiday Inn column shear damage from 1994 Northridge EQ

Specimen configuration

- ✓ 21 columns are selected from experimental tests.[flexure-shear failure (FSC):8, flexure failure (FC):4, shear failure (FC):9]
- ✓ Columns were experimentally tested at full-scale under various loading protocols.
- ✓ All tested columns used for calibration sustained axial collapse.
- ✓ Selected columns covered a practical range of axial loads, shear stresses, transverse reinforcement ratios, longitudinal reinforcement ratios, and shear span to depth ratios.

Specimen name	Author	Type of failure	Section dimension (height width) mm	Clear height mm	Shear span/depth ratio (a/d)	Tie hook angle	Tie spacing mm	Transv. reinf. ratio $A_v / b_w * s$	Long. reinf. ratio $A_s / b_w * h$
Specimen_1	Sezen	FSC	457x457	2,946	3.76	90	304.8	0.002	0.02
SC-2.4-0.2	Tran	SC	350.5x350.5	1,700	2.80	135	124.9	0.001	0.02
1NL	Li	SC	500x300	498	0.60	135	200	0.002	0.04
CH100	Sokoli	FC	457x457	2,743	3.35	90	89	0.009	0.01



FS-Specimen_4 (Low axial load-Monotonic)

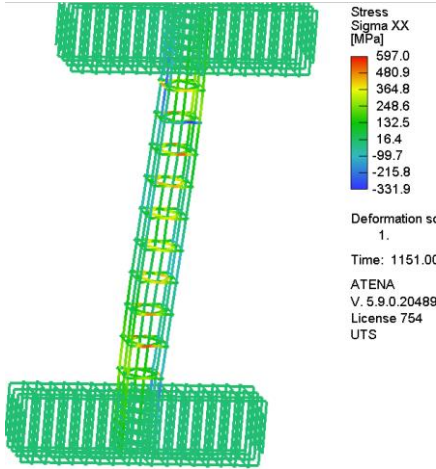
Simulated deformed shape and crack patterns



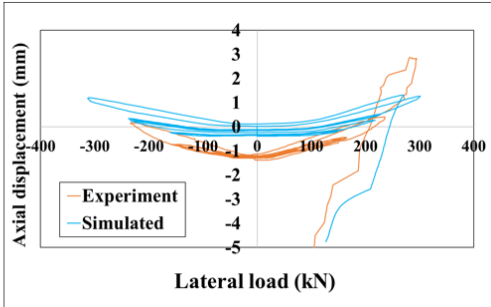
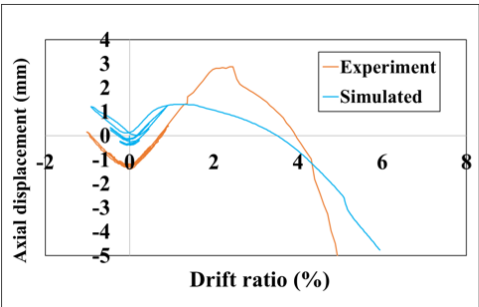
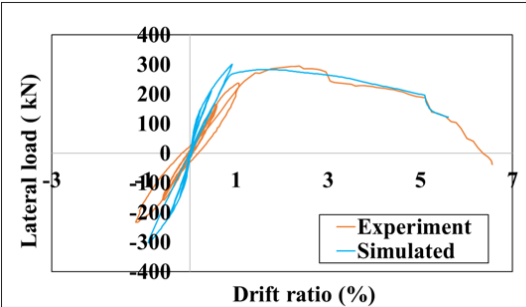
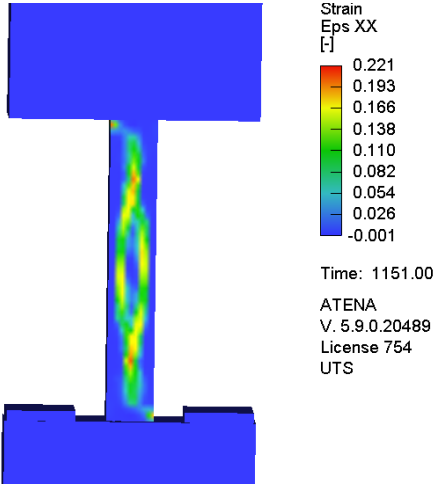
Experimental deformed shape



Reinforcement deformed shape and Stress(MPa)



Concrete strain



FS- Specimen_1 (Low axial load-Three-cycle)

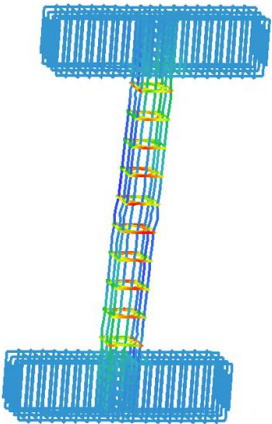
Simulated deformed shape and crack patterns



Experimental deformed shape

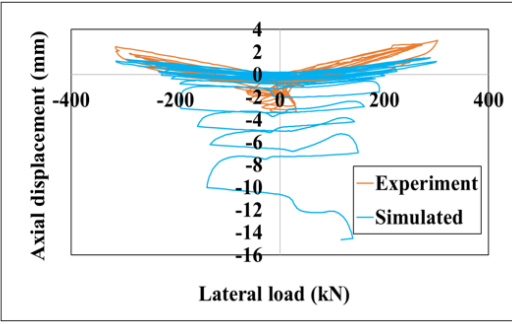
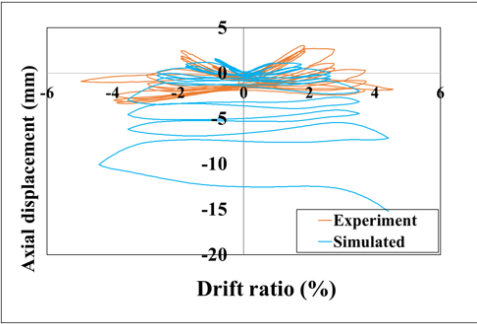
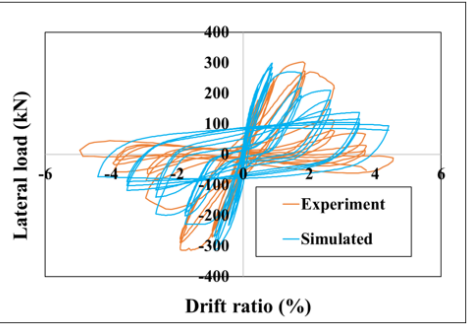
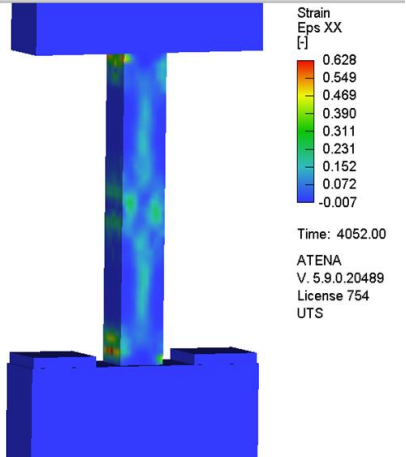


Reinforcement deformed shape and Stress(MPa)



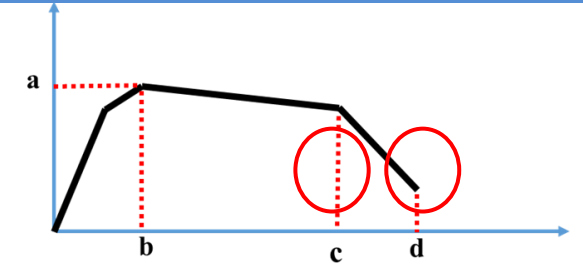
Stress
Sigma XX
[MPa]
713.5
604.1
494.7
385.4
276.0
166.7
57.3
-52.1
-161.4
Deformation scale
1.
Time: 4052.00
ATENA
V. 5.9.0.20489
License 754
UTS

Concrete strain



Simulation Error

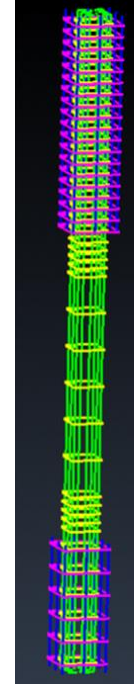
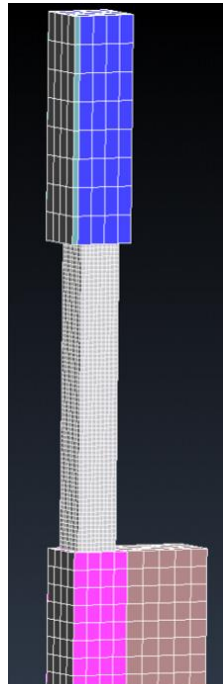
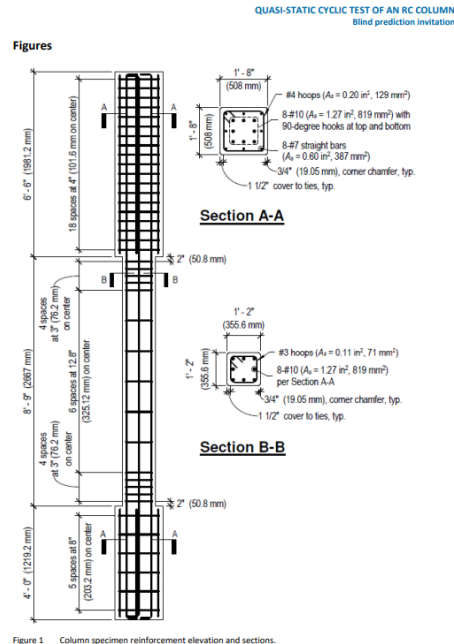
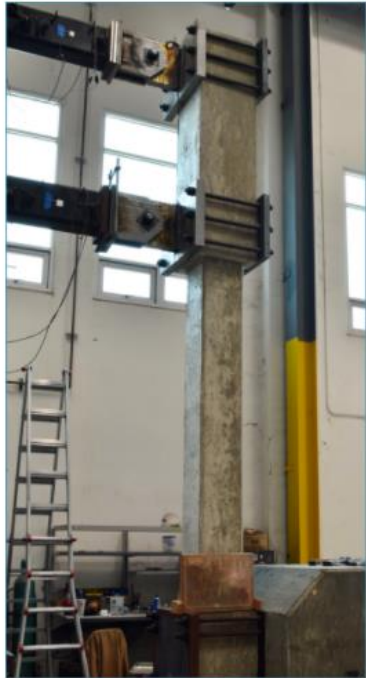
Column name	NE* peak lateral strength (%)	NE drift ratio at capping point (%)	NE drift ratio at axial degradation (%)
3CLH18	4	0	0
3CMH18	5	0	0
SC-2.4-0.2	2	18	1
SC-2.4-0.5	11	0	6
Specimen#1	12	0	0
Specimen#2	5	-8	-4
1NL	1	11	NA
2NL	2	12	NA
2NH	11	14	NA
CS60	2	6	0
CS80	11	0	0
Specimen_1	5	15	2
Specimen_2	10	20	0
Specimen_4	2	12	0
2L06	1	6	1
2 H06	5	0	1
3CMD12	2	9	1
CH60	1	2	1
CH100	2	1	0
Mono	1	1	2
CYC	7	0	0



$$NE = \text{Normlized Error} = \frac{\text{Experimental value} - \text{Simulation value}}{\text{Experimental value}} \times 100$$

Model accuracy

Winner of the blind prediction contest at PEER (Pacific Earthquake Engineering Research Center) 2021 RC Column Blind Prediction at UC Berkeley among 40 counters and more than 120 applicants



Shear strength model	Predicted or actual strength
ASCE 41-17, Equation 10.3	12 kips
ASCE 41-17, Equation 10, omitting tie spacing requirement	23 kips
ACI 318-19	30 kips
My prediction	40.6 kips
Test result	40 kips



THE WORLD'S GATHERING PLACE FOR ADVANCING CONCRETE

aci CONCRETE CONVENTION

Simulations under various lateral protocols and axial loads

✓ 116 simulations were conducted using the 18 column models.

Loading	Number of cycles at each amplitude	Column lateral drift ratio (%)
Monotonic	Three cycles at the first two, push over	0.25, 0.5, push over until axial failure
One-cycle	1	0.25, 0.5, 1, 1.5, 2, 2.5, 3, 4,5,6,7,8, axial failure
Three-cycle	3	0.25, 0.5, 1, 1.5, 2, 2.5, 3, 4,5,6,7,8, axial failure
Six-cycle	6	0.25, 0.5, 1, 1.5, 2, 2.5, 3, 4,5,6,7,8, axial failure

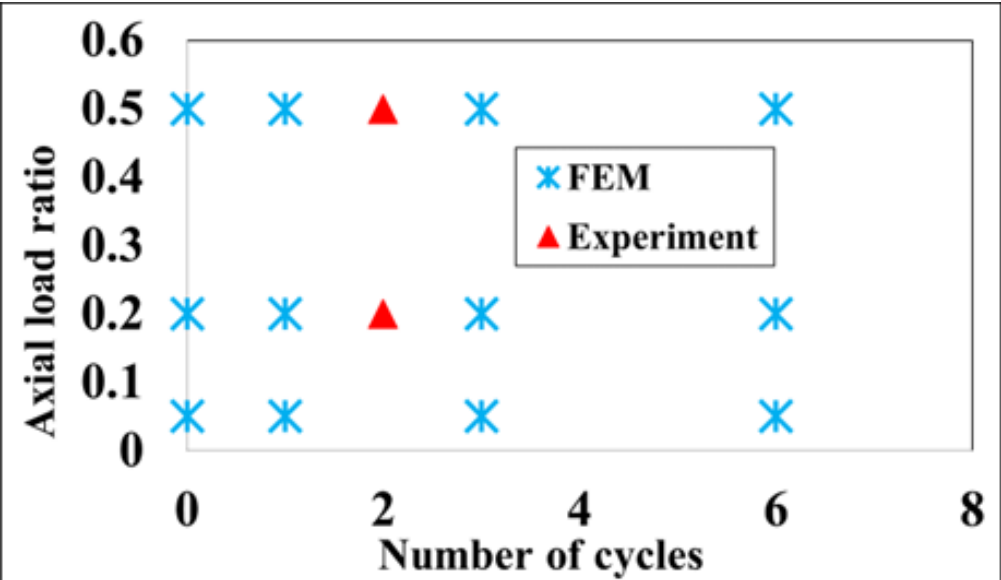
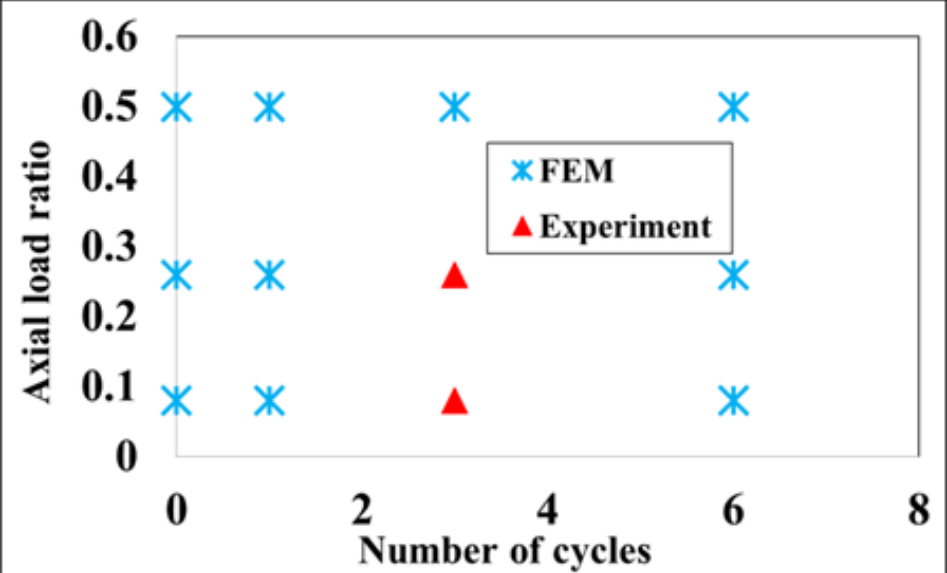
→ Applied lateral load

Column name	Axial load ratio
CH60	0.05, 0.15, 0.25, 0.5
SC-2.4	0.05, 0.2, 0.5
3CLH18	0.08, 0.26, 0.5
Specimen_1	0.05, 0.15, 0.6
2L06	0.05, 0.18, 0.4
CS60	0.05, 0.29, 0.5
Speimen#1	0.05, 0.36, 0.5
Speimen#2	0.05, 0.37, 0.5
CS80	0.27
3CMD12	0.27
CH100	0.15
CYC	0

→ Applied axial load

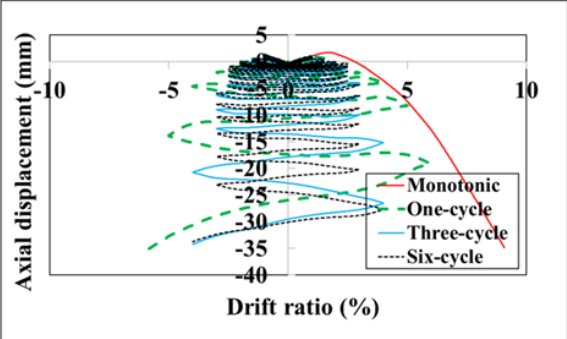
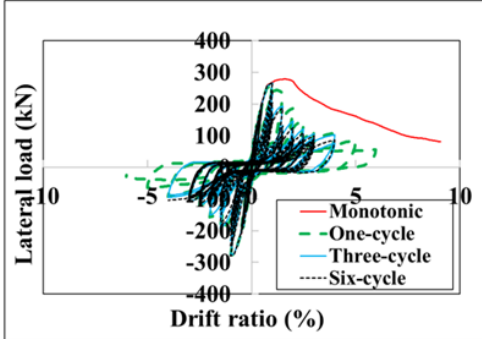


Simulations under various lateral protocols and axial loads (sample)

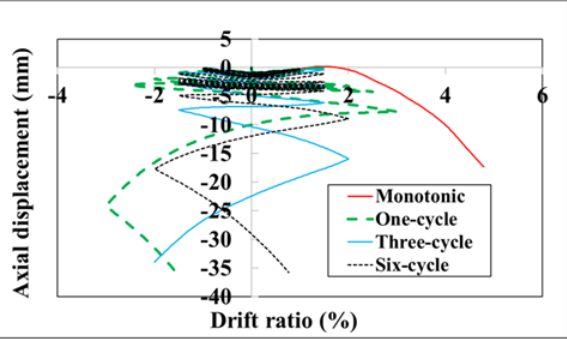
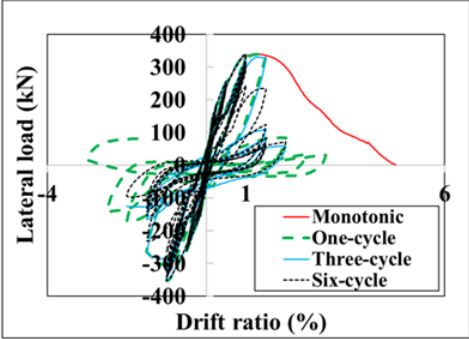


Sample column, FEM loading vs Experimental loading

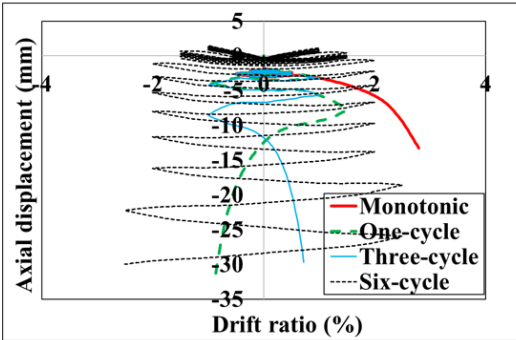
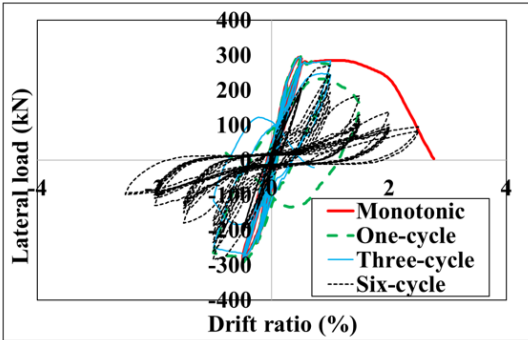
Simulations under various lateral protocols and axial loads (3CLH18- SC)



Axial load ratio of 0.08



Axial load ratio of 0.26



Axial load ratio of 0.5



Parameters for drift capacity relations

$$\Delta_{capping} = \left(\frac{DR_{capping-Cyc}}{DR_{capping-Mono}} \right)$$

$$\Delta_{axial} = \left(\frac{DR_{axial-Cyc}}{DR_{axial-Mono}} \right)$$



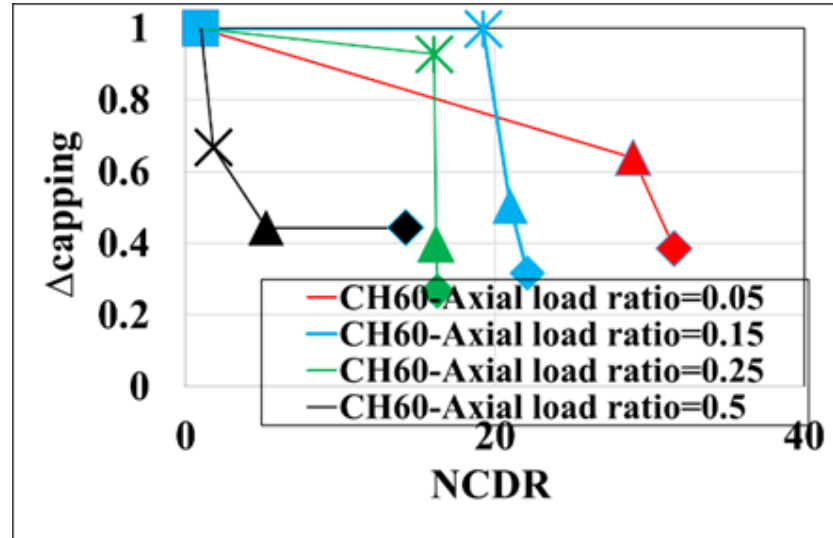
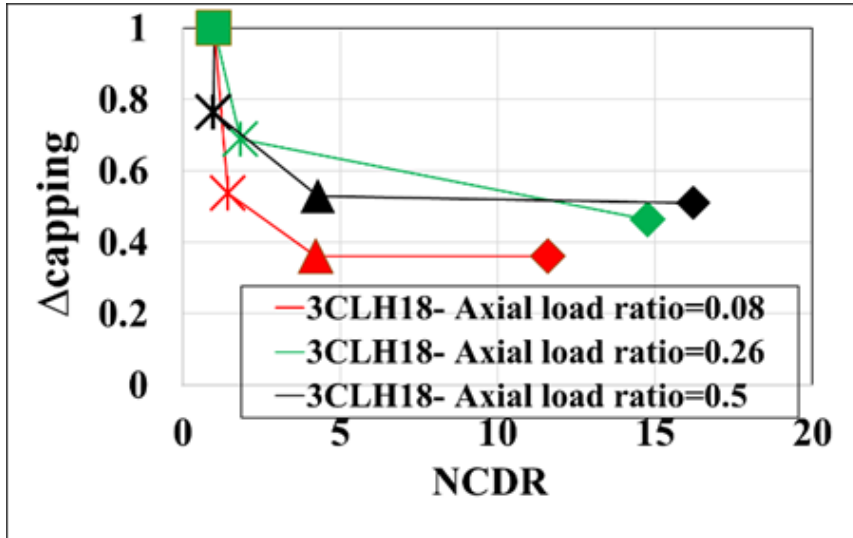
Response variables

$$\text{Normalized cumulative drift ratio (NCDR)} = \frac{\text{Cumulative drift ratio } f \text{ cyclic}}{\text{Cumulative drift ratio } f \text{ monotonic}}$$



Predictor Variables Related to Loading History

✓ $\Delta_{capping}$ vs NCDR for 3CLH18 and CH60 (square marker = monotonic loading, cross marker = One-cycle protocol, triangle marker = Three-cycle protocol, diamond marker = Six-cycle protocol)



Proposed drift capacity equations

- ✓ Lasso regression analyses were conducted to arrive at equations for $\beta_{\text{capping}} - \text{NCDR}$ and $\beta_{\text{axial}} - \text{NCDR}$
- ✓ ρ_l represents the longitudinal reinforcement ratio, and $\left(\frac{P}{f'_c * Ag}\right)$ represents the axial load ratio
- ✓ Increasing the axial load ratio therefore reduces β , which results in smaller values for Δ_{axial} and therefore sharper drops in drift capacity at axial degradation with increasing cycles.
- ✓ The axial load ratio has an opposite effect on the capping point, with an increase causing β to become larger, resulting in a larger Δ_{capping} .
- ✓ Higher ρ_l values increase the damaging effect of lateral cycles dropping drift capacities from monotonic ones more sharply than for low ρ_l values.
- ✓ An increase in (ρ_l) tends to increase the shear demand on columns, which may contribute to the larger effects of lateral cycling on drift capacities.

$$\beta_{\text{capping-NCDR}} = -0.23\rho_l + 0.16\frac{P}{f'_c * Ag} \leq 0.0$$

$$\beta_{\text{axial-NCDR}} = -0.08\rho_l - 0.23\frac{P}{f'_c * Ag} \leq 0.0$$

Validation

- ✓ Specimen_1 and Specimen_4 are selected to validate the proposed drift capacity equations.
- ✓ Specimen_1 was experimentally tested under cyclic loading (three cycles per drift amplitude), while its nominally identical counterpart Specimen_4 was tested under monotonic loading.
- ✓ Both columns were subjected to the same axial load ratio of 0.15.
- ✓ The drift capacities for capping and axial degradation for Specimen_1 and Specimen_4 obtained experimentally
- ✓ The estimation of the capping point and axial degradation drift capacities under monotonic loading are seen to be conservative compared with experimental values.
- ✓ This is partly due to having several column simulations reaching 10% drift ratio without experiencing lateral or axial strength degradation.

Method	Cyclic loading, drift ratio for capping point (%)	Monotonic loading, drift ratio for capping point (%)	Cyclic loading, drift ratio for axial degradation (%)	Monotonic loading, drift ratio for axial degradation (%)
Experiment	2.76	3.1	4.96	6.45
Drift based equation	N.A.	2.76	N.A.	5.60



Example application with ACI 369.1- ASCE 41-17 drift capacities

- ✓ The drift capacities of Specimen_1 are first calculated from ACI 369.1-22 modelling parameters a_{nl} , representing the capping point and b_{nl} representing the axial degradation point
- ✓ The corresponding NCDR were evaluated using the Three-cycle drift protocol
- ✓ Equations provided a conservative increase in drift capacity when adjusting loading protocol from cyclic to monotonic loading by about 10 to 15%
- ✓ ACI 369.1-22 provides reasonably accurate estimates of drift capacities for the column considering under cycling loading

Method	Cyclic loading, drift ratio for capping point (%)	Monotonic loading, drift ratio for capping point (%)	Cyclic loading, drift ratio for axial degradation (%)	Monotonic loading, drift ratio for axial degradation (%)
Specimen-1 or Specimen_4 (Experiment)	2.76	3.1	4.96	6.45
ACI 369.1-22	2.5	N.A.	5.3	N.A.
Drift based equation	N.A.	2.5	N.A.	5.6

Conclusion

- ✓ 21 reinforced concrete columns were calibrated to experimental data with a FEA software ATENA where the parameters were optimized and selected
- ✓ Modl parameters were proposed for FE modeling of FC, FSC, and SC columns up to collapse.
- ✓ Using the recommended modeling parameters, FE models produced relatively accurate estimates of columns behavior, errors did not 5% compared with test data in most cases
- ✓ 18 calibrated models, we subjected to 4 types of lateral loading protocol under three axial load levels: low (0-0.15), moderate (0.15-0.35), and high (0.36-0.6). In all, 116 simulations were conducted using the 18 column models.
- ✓ Increasing axial load increased the effect of cycles on the drift ratio at axial strength loss, which is the opposite from lateral strength loss, for which a higher axial load reduces the effects of cycles.
- ✓ In addition, axial degradation was found to initiate for columns with moderate to high axial load loading when columns lateral strength is close to zero,
- ✓ Relations are proposed that estimate changes in drift capacities due to lateral cycling.
- ✓ The relations are intended to transform a drift capacity obtained either experimentally or from a standard into an estimate of the drift capacity for a different loading protocol.

Thank you

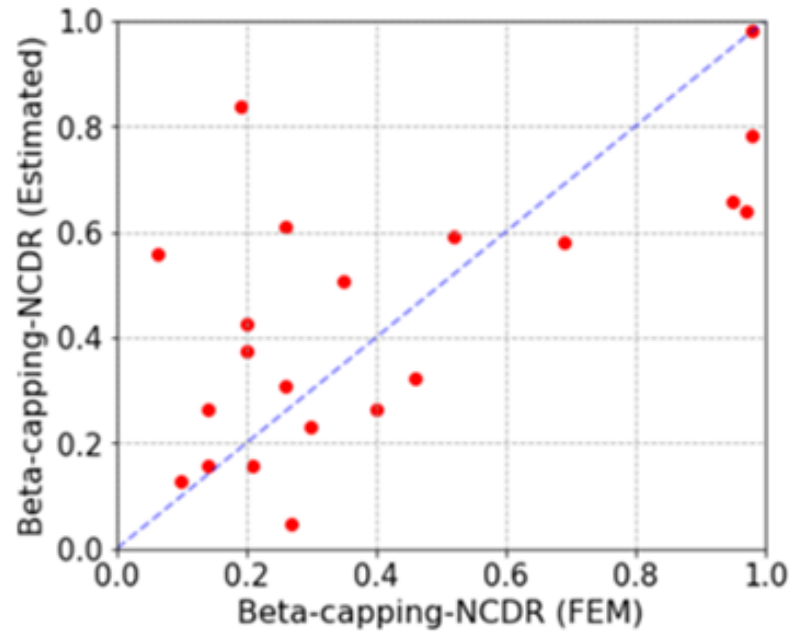
THE WORLD'S GATHERING PLACE FOR ADVANCING CONCRETE

 **CONCRETE
CONVENTION**

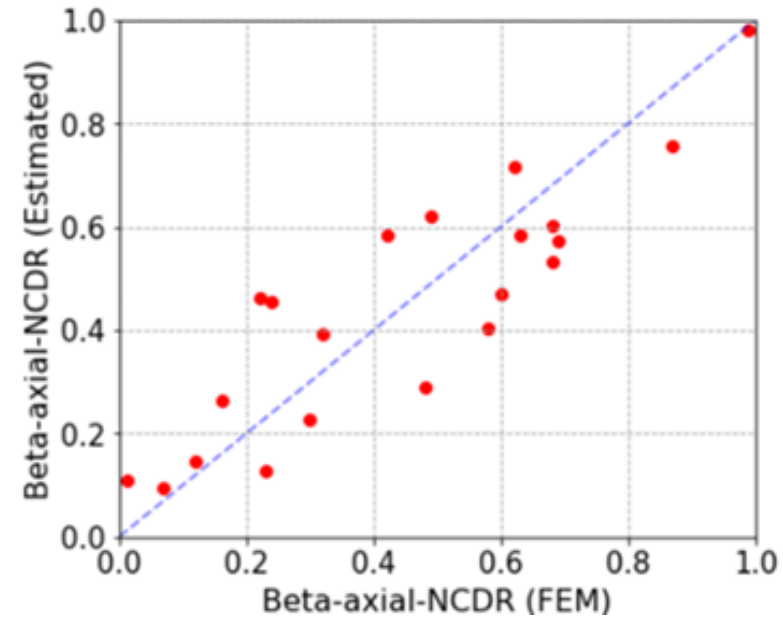


Proposed drift capacity equations

- ✓ Regression estimates for β versus β values from FE analyses for capping point axial failure



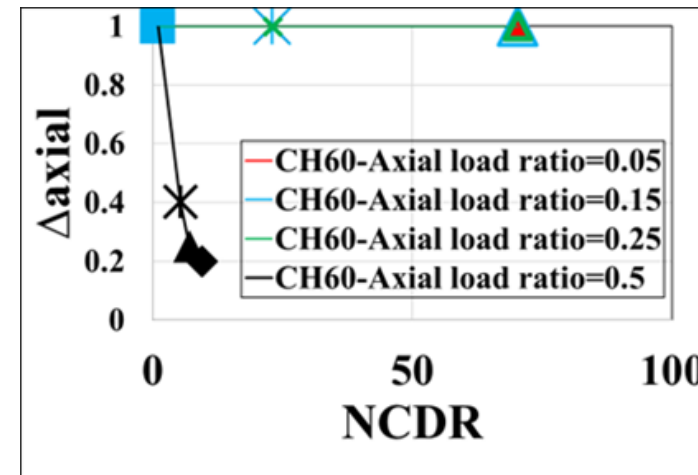
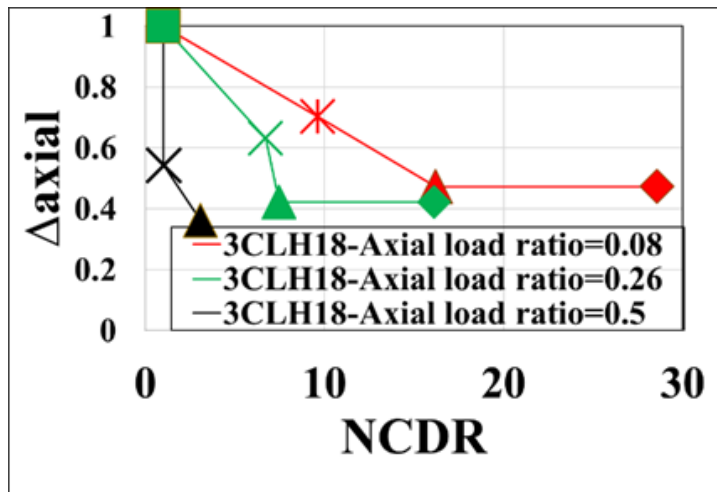
$$R^2 = 0.6$$



$$R^2 = 0.8$$

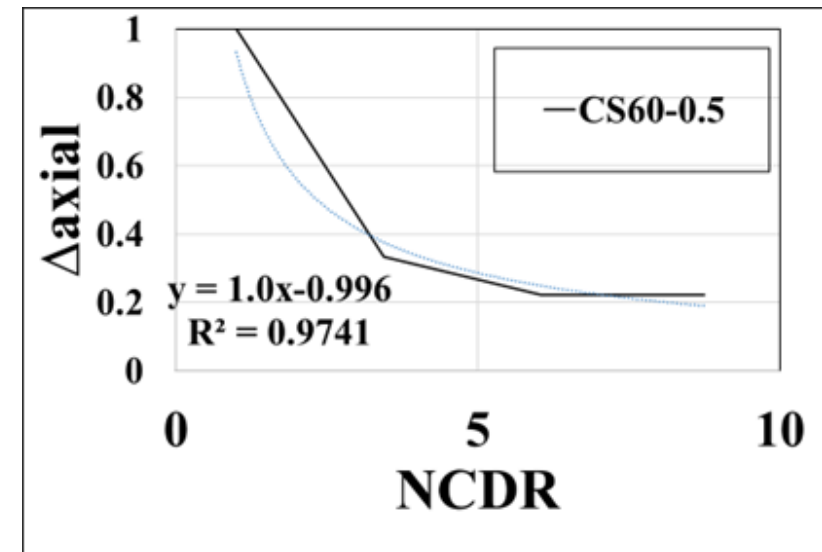
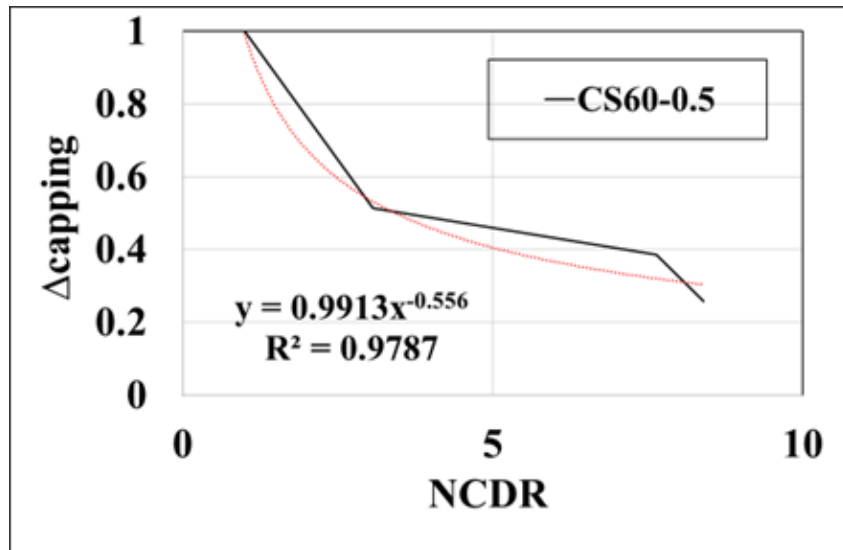
Parameters for drift capacity relations

- ✓ Most columns under a low axial load ratio (0-0.15) that are subjected to different lateral loading protocols reach 10% drift ratio before reaching the defined axial failure point (1% axial shortening). This behavior is more prominent in columns with a higher amount of confinement (CH60, CYC, CH100) or columns under lower shear stresses (Specimen_1, Specimen_2).
- ✓ For columns with higher axial load ratios, the axial load ratio appears to reduce Δ_{axial} , such that lateral cycles decrease drift capacity at axial failure more rapidly under higher axial loads.
- ✓ The capping point deformation capacity has an opposite trend whereby columns under a higher axial load ratio experience a larger $\Delta_{capping}$, which indicates that increasing axial load ratio reduces the effect of cycles on the capping point



Drift capacity relations

- ✓ α adjusts the intercept of the relation, while a negative β changes the rate of decay for $\Delta_{capping}$ or Δ_{axial} .
- ✓ Since NCDR is normalized to demands under monotonic loading, α in the equations is always 1.0.
- ✓ When $\beta = 0$, columns have the same drift capacity monotonic or cyclic loading regardless of number of cycles, resulting in $\Delta = \alpha = 1.0$



$$\Delta_{capping-NCDR} = \frac{DR_{capping-Cyc}}{DR_{capping-Mono}} = \alpha \times (NCDR)^{\beta_{capping-NCDR}}$$

$$\Delta_{axial-NCDR} = \frac{DR_{axial-Cyc}}{DR_{axial-Mono}} = \alpha \times (NCDR)^{\beta_{axial-NCDR}}$$



Drift capacity relations

✓ β parameters are derived for each column and axial load ratio for the capping point and axial failure point

Column name	Axial load	β capping-NCDR	β axial-NCDR
SC-2.4-0.2	0.05	-0.50	-0.01
	0.2	-0.47	-0.48
	0.5	-0.46	-0.49
3CLH18	0.08	-0.36	-0.23
	0.26	-0.26	-0.32
	0.5	-0.20	-0.62

Application of drift capacity equations

- ✓ The proposed drift capacity equations can be used to adjust column drift capacities from a cyclic protocol to a monotonic and vice versa for both capping point and axial degradation

From cyclic to monotonic

$$(DR_{capping-Mono})^{(\beta_{capping-NCDR}-1)} = \frac{(CDR_{Cyc})^{\beta_{capping-NCDR}}}{DR_{capping-Cyc}}$$

From monotonic to cyclic

$$DR_{capping-Cyc} = \frac{(CDR_{Cyc})^{\beta_{capping-NCDR}}}{(DR_{capping-Mono})^{(\beta_{capping-NCDR}-1)}}$$

Drift capacity relations

- ✓ The parameters with lowest p-values with respect to $\beta_{\text{capping}} - \text{NCDR}$ and $\beta_{\text{axial}} - \text{NCDR}$ are ρ_l and axial load ratio.
- ✓ Axial load ratio appears as a primary parameter influencing changes in drift capacity of concrete columns due to cyclic loading for axial points

	p – values $\beta_{\text{capping}} - \text{NCDR}$	p – values $\beta_{\text{axial}} - \text{NCDR}$
ρ_t	0.910	0.584
ρ_l	0.044	0.024
Axial load ratio	0.149	1.4E-06